Peer Reviewed Paper openaccess

An identification method for defective tablets by distribution analysis of near infrared imaging

Daitaro Ishikawa,[a,*] Kodai Murayama,[b] Takuma Genkawa,[c] Yuma Kitagawa[b] and Yukihiro Ozaki[d]

[a]Faculty of Agricultural Sciences, Fukushima University, 1 Kanayagawa, Fukushima 960-1296, Japan.
E-mail: daitaroishikawa@agri.fukushima-u.ac.jp

[b]Research and Development Department, Yokogawa Electric Corporation, 2-9-32 Nakacho, Musashino, Tokyo 180-8750, Japan

[c]Food Research Institute, NARO, 2-1-12 Kannondai, Tsukuba, Ibaraki 305-8642, Japan

[d]School of Science and Technology, Kwansei Gakuin University, 2-1 Gakuen, Sanda, Hyogo 669-1337, Japan

The present study aims to suggest a method to identify defective tablets by near infrared (NIR) imaging. A newly developed portable imaging system (D-NIRs) was used in this study, in which the spectrometer is equipped with a high-density photodiode array detector to record high-quality spectra with 1.25 nm spectral resolution. This system is highly portable and allows an image of a target tablet to be developed in approximately 10 s. Normal tablets containing 0.1–20% magnesium stearate, ascorbic acid, corn starch and talc were prepared. NIR spectra in the 950–1700 nm region of each pixel in a tablet were measured, and NIR images were generated from the second derivative of the spectra at 1213 nm. It was confirmed that the spectral distribution in a tablet passed as a normal distribution by the goodness-of-fit test ($p \leq 0.05$). Consequently, the average of the spectra obtained from each pixel of the whole tablet was used to predict the concentration of magnesium stearate. The quantitative accuracy of the prediction model by the second derivative spectra achieved $R^2 = 0.931$ and RMSE = 1.90%. Defective tablets were prepared with localised magnesium stearate. The skewness of the second derivative in the defective tablet was larger than that of the standard distribution. Specifically, the distribution of defective tablets was biased to the right as compared to the standard distribution. The results of the presented study suggest that spectral imaging combined with distribution analysis is an effective method to identify defective tablets.

Keywords: NIR spectroscopy, defective tablet, distribution analysis, skewness, NIR imaging

Introduction

Process analytical technology (PAT) is a comprehensive control mechanism for pharmaceutical production, involving production design, process analysis and management.[1–4] Numerous studies have been performed to characterise pharmaceutical tablets by various spectroscopic and imaging techniques.[5–11] Identification of defective tablets is essential for quality control by PAT in the pharmaceutical industry. Because process monitoring requires the evaluation of inhomogeneity of compounds in a tablet, the intro-

Correspondence
D. Ishikawa (daitaroishikawa@agri.fukushima-u.ac.jp)

Received: 26 January 2019
Revised: 19 June 2019
Accepted: 25 July 2019
Publication: 13 August 2019
doi: 10.1255/jsi.2019.a15
ISSN: 2040-4565

Citation
D. Ishikawa, K. Murayama, T. Genkawa, Y. Kitagawa and Y. Ozaki, "An identification method for defective tablets by distribution analysis of near infrared imaging", *J. Spectral Imaging* **8,** a15 (2019).
https://doi.org/10.1255/jsi.2019.a15

duction of imaging technology can be beneficial to this.

Visual inspection of process monitoring is one of the most effective methods for detecting a defective tablet.[12,13] Although an image in the visible region is adequate to detect physical defects for many applications, it cannot always provide information about the defective concentration distribution. Therefore, NIR chemical imaging can be a useful tool to investigate the inhomogeneity of components in pharmaceutical tablets.[14–16] A classification method combined with principal component analysis (PCA) was suggested in the literature for the identification of counterfeit tablets.[17,18] Wu *et al.* have demonstrated that NIR imaging was a promising technology for visualising the spatial distribution and homogeneity.[19] The proposed PCA methodology provides a means to gain an understanding of the process by inspecting the main sources of variation in the hyperspectral images. Moreover, research has led to improvements in the development of process control methods using multivariate analysis such as partial least squares (PLS) regression.[20–23] Khorasani developed an API distribution and content for both roller-compacted ribbons and tablets using NIR imaging combined with in-line PCA and PLS models.[20] The good quantitative result of Mg-stearate and API in a tablet has also been reported by using CLS and MCR-ALS.[23]

NIR imaging devices and systems that can be utilised for in-line or at-line process control are being developed simultaneously, because the potential of NIR imaging strongly relies on the performance of the NIR imaging device. In the past decade, powerful NIR imaging devices and systems have been presented, and the efficiency of NIR imaging has led to it being evaluated for pharmaceutical applications.[7,24–26] We developed a portable NIR imaging device, D-NIRs.[27,28] For an 8 mm tablet sample, D-NIRs can monitor two-dimensional spectra in the 900–1700 nm region within 5 s. D-NIRs' potential as a PAT tool has been discussed in previous studies,[29–31] which have demonstrated that the concentration of components in a tablet can be estimated by D-NIRs with high quantitative accuracy. We found that D-NIRs is useful to determine the optimised blending period of pharmaceutical samples.[31] Additionally, D-NIRs can be used as a Quality by Design tool to monitor the dissolution process of a tablet. We also demonstrated that a spectral image produced from the ratio index of the second derivatives at 1361 nm and 1354 nm was effective in evaluating the dissolution of a tablet.[32]

Results of NIR imaging research have frequently shown an expansion of spectral analysis for a point on the tablet. In other words, as a consequence of spectral analysis, an image developed from the arbitrary object has been used as supplementary information. It is, therefore, expected that an approach from an image analysis technology standpoint creates new potential for the field of spectroscopic imaging.

One can find that histogram statistics such as kurtosis and skewness are useful in the assessment of a defective object. Although most researchers have calculated these histogram statistics,[33] their potential as tablet quality evaluation methods has not been discussed thoroughly.[19]

Sacré *et al.* described the limitations of investigating the spatial distribution of the object in a tablet using histogram statistics;[34] namely, histogram statistics provide information about the homogeneity of a compound, however, the spatial information is not considered. Thus, most recently, alternative methods such as micropixel analysis have been suggested to monitor the blending process.[35] Nevertheless, the use of histogram statistics as the standard of evaluation still seems advantageous to objectively evaluate the distribution of a component in a tablet.

The present study was performed to propose a method to evaluate the tablet quality using chemical imaging technology combined with image analysis. For image analysis, we first examined the normality of spectral distribution in a tablet by the Chi-square (χ^2) goodness-of-fit test, and then tried to quantitatively evaluate the tablet quality by comparing it with a defective tablet.

Instrumentation

D-NIRs consists of a polychromator type spectrometer (P-NIRs), an imaging unit and a halogen light source.[27] The diffuse reflection energy of a sample reaches the D-NIRs imaging unit, which is equipped with two galvano mirrors that obtain two-dimensional data (in the X- and Y-directions). In its current phase of development, D-NIRs can perform two-dimensional measurement in the 950–1700 nm region with 0.1 mm of maximum spatial resolution. The spectral data are obtained by P-NIRs connected to the imaging unit using a fibre probe. P-NIRs has also been developed by our group for process monitoring in the pharmaceutical field.[28] The spectrometer is equipped with a newly developed high-density photodiode array detector of 640 elements with a 20 µm

pitch. An indium gallium arsenide (InGaAs) photodiode is used in this spectrometer and has sensitivity in the 900–1700 nm region and can measure a target spectrum in 1.25 nm intervals in that region. A silicon integrated circuit type charge amplifier array has also been developed to amplify the converted photocurrent by the elements. The use of a newly developed photodiode array (PDA) detector combined with this amplifier contributes strongly to the high-speed monitoring: it takes less than 10 ms to obtain a spectrum. Consequently, two-dimensional spectral data of an NIR image of a sample tablet (⌀8.0 mm) are obtained within 14 s by our system. The characteristics of D-NIRs and its applications have been reported elsewhere.[27,28] Although we have not yet published this information, a 5 s D-NIRs monitoring time has been achieved.

Material and methods

Sample preparation

Powders of 5 wt% ascorbic acid, 5 wt% talc, 0.1–20 wt% magnesium stearate (Mg-stearate) and corn starch were purchased from Kanto Chemical Co, Ltd (Tokyo, Japan) and Wako Pure Chemical Industries, Ltd (Osaka, Japan) as materials for sample tablets. They were mixed and pressed at 10 MPa by a tableting machine (Handtab-100, Ichihashi Seiki Co. Ltd, Kyoto, Japan). The prepared tablets were flat, and their diameter and thickness were 8.0 and 1.0 mm, respectively.

A model sample of the defective tablet was prepared by adding Mg-stearate to a sample tablet containing 5 wt% Mg-stearate. Mg-stearate was added to 12.5, 25 and 50 % of the surface area of the sample tablet and pressed once more at 10 MPa by the tableting machine.

Spectral collection

A point spectrum in the $10 \times 10\,mm^2$ area, including a sample tablet, was obtained by D-NIRs. The NIR spectra in the 900–1700 nm region were measured at 1.25 nm intervals; the spatial resolution was 0.5 mm. Integration time of a point measurement was 20 ms.

The spectra obtained from a tablet were transcribed to text format, and Unscrambler (version 10.3, CAMO Software AS) was used for spectral analysis. The spectra were subjected to second derivative smoothing, including Savitzky–Golay smoothing (31 point and 2nd order), to determine the informative peaks for mapping.[36]

Distribution analysis for identification of defective parts

To evaluate the distribution of spectral intensity in a tablet, the χ^2 goodness-of-fit test for normal distribution was attempted on the spectra data of non-defective tablets. The goodness-of-fit test is a method for examining the goodness-of-fit by applying a probability distribution in sample data. We examined the correspondence of the spectral intensity distribution of a sample tablet to the normal distribution as a probability distribution with the aim of quantifying the distribution standard. The intensity obtained from each point in a tablet is compared with the expected value from the normal distribution of tablet components. The null hypothesis of the test statistic can describe that the sample distribution follows the normal distribution, whereas the alternative hypothesis can describe that the sample distribution does not follow the normal distribution. If the statistic value of χ^2 obtained from the samples is sufficiently large, the alternative hypothesis is accepted. In this study, the significant level was set to $p \le 0.05$.

The distribution characteristics of spectral intensity between a defective tablet and a non-defective tablet were compared by skewness as follows:

$$\text{skew} = \frac{1}{N}\sum_{j=1}^{N}\left[\frac{x_j - \overline{x}}{\sigma}\right]^3 \quad (x_1 \ldots x_N)$$

where N is the number of pixels in an image, x_j is an intensity at the point j, $\overline{x}$ is the average of intensity in a tablet and σ is the standard deviation of intensity in a tablet. Note that the skewness is the third moment about the mean, and it indicates distribution symmetry.

Results and discussion

NIR spectra of ascorbic acid, Mg-stearate, corn starch and talc in powder forms

Figure 1 shows NIR spectra of ascorbic acid, Mg-stearate, corn starch and talc in powder forms, in the 1000–1700 nm region. Bands at 1360 nm and 1458 nm of ascorbic acid may be assigned to the first overtones of stretching vibrations of free and intermolecular hydrogen–bonded OH groups, respectively.[37] Bands in the 1150–1250 nm region of ascorbic acid and corn starch are due to CH stretching vibrations.[38] A sharp peak at 1391 nm of talc arises from the OH stretching vibration mode.[38] Mg-stearate yields

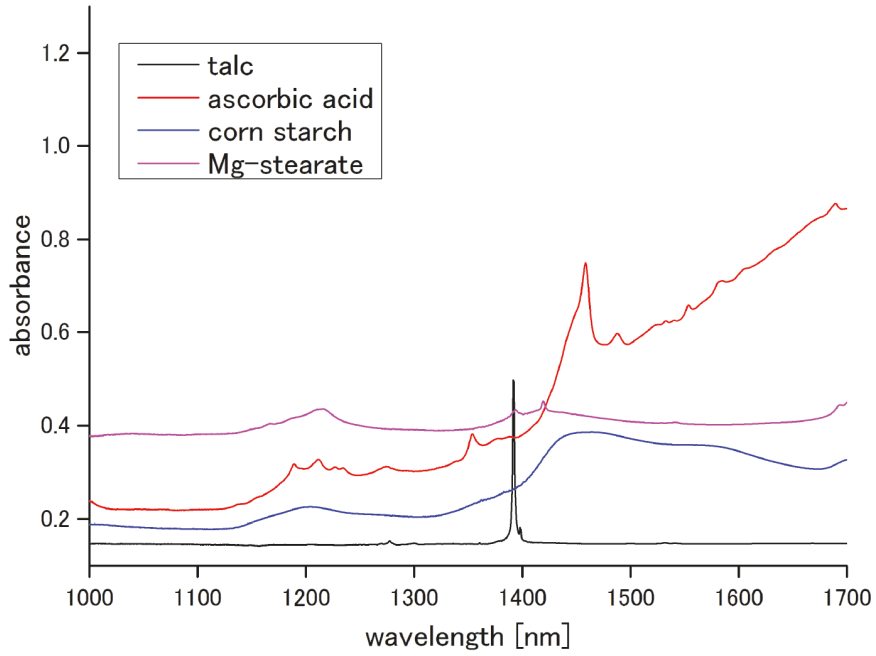

Figure 1. Absorbance of ascorbic acid, Mg-stearate, talc and corn starch in powder form. Note that the spectra of Figure 1 were obtained with a VECTOR 22/N (Bruker Optics, Germany) as references of the band assignment.

three peaks at around 1213, 1394 and 1413 nm. These peaks may originate from CH stretching and a combination of νCH_2 and σCH_2, respectively.[39]

Distribution of the concentration for Mg-stearate in a non-defective tablet

Figures 2(a) and 2(b) show NIR spectra in the 1000–1700 nm region and the second derivative spectra of tablet samples with 0.1–20% Mg-stearate. Note that the spectra were measured at the centre of each tablet. An absorbance band was observed in the range of 1150–1250 nm, and the maximum absorbance was found to be located around 0.3–0.35 in the 1450–1500 nm region. The absorbance was found to decrease in the longer wavelength region. The three peaks at around 1213, 1391 and 1417 nm in the second derivative spectra varied according to the change in the concentration of Mg-stearate. As described above, although the peaks at 1391 and 1417 nm were assigned to combination modes of CH_2, they overlapped with the other peaks generated from ascorbic acid, talc and corn starch. Consequently, a peak at around 1213 nm was selected to quantify the concentration of Mg-stearate.

NIR images developed by the second derivative method at 1213 nm are shown in Figure 3. False colour in the tablets gradually changes with the concentration of Mg-stearate. However, it is simultaneously seen that the colour in each tablet is inhomogeneous. Figure 4 shows the distribution of the second derivative value in each tablet. Note that the histograms are drawn using standardised data by the mean and standard deviations of second derivative spectra in a tablet. The value obtained from each tablet agrees well with the standard distribution of mean = 0 and variance = 1. As shown in Table 1, the statistic parameter χ^2 calculated for the goodness-of-fit test is between 10.87 and 26.35 for a tablet containing 0.1–20% Mg-stearate. As all calculated values were lower than 27.587 ($n = 17$) at significance level $\alpha = 0.05$, the null hypothesis of the test statistic remains. In other words, it demonstrates that the distribution of second derivative spectra in a non-defective tablet could be described by a normal distribution without dependence on concentration. Therefore, the average of the second derivative obtained from each pixel in a tablet could be used to quantify the concentration of Mg-stearate as a representative value. The quantitative accuracy of Mg-stearate obtained by an average of the second derivative at 1213 nm was $R^2 = 0.931$ and RMSE = 1.90%. The accuracy was improved to $R^2 = 0.998$ and RMSE = 0.78% by a PLS regression model combined

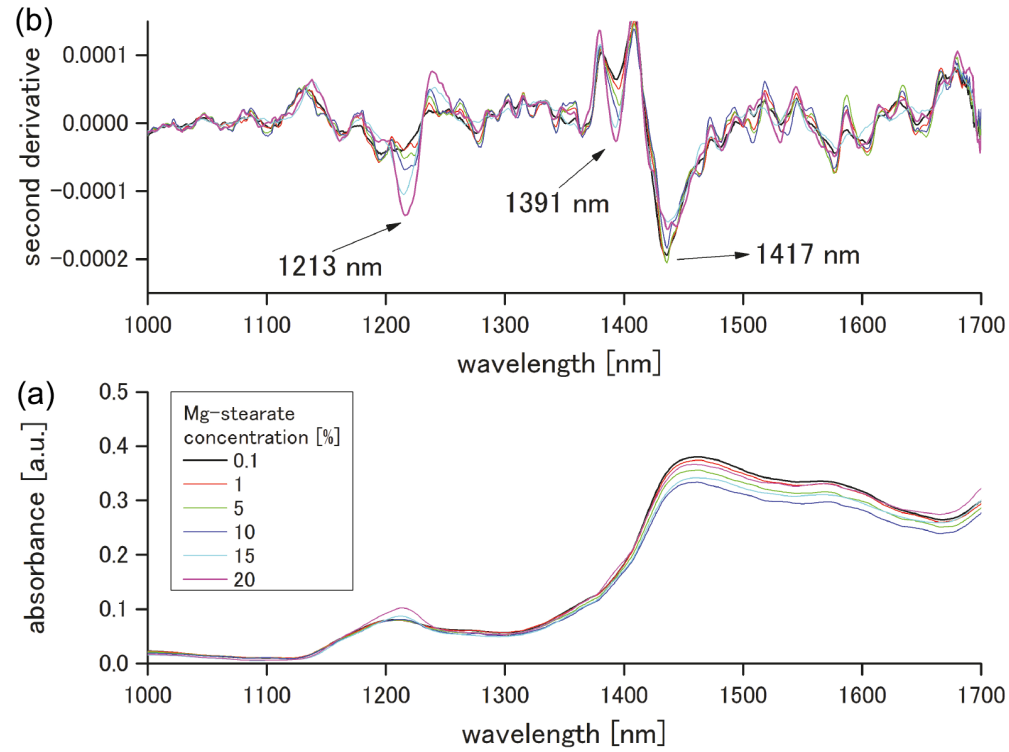

Figure 2. (a) NIR spectra and (b) their second derivative spectra of sample tablets with 0.1–20% Mg-stearate.

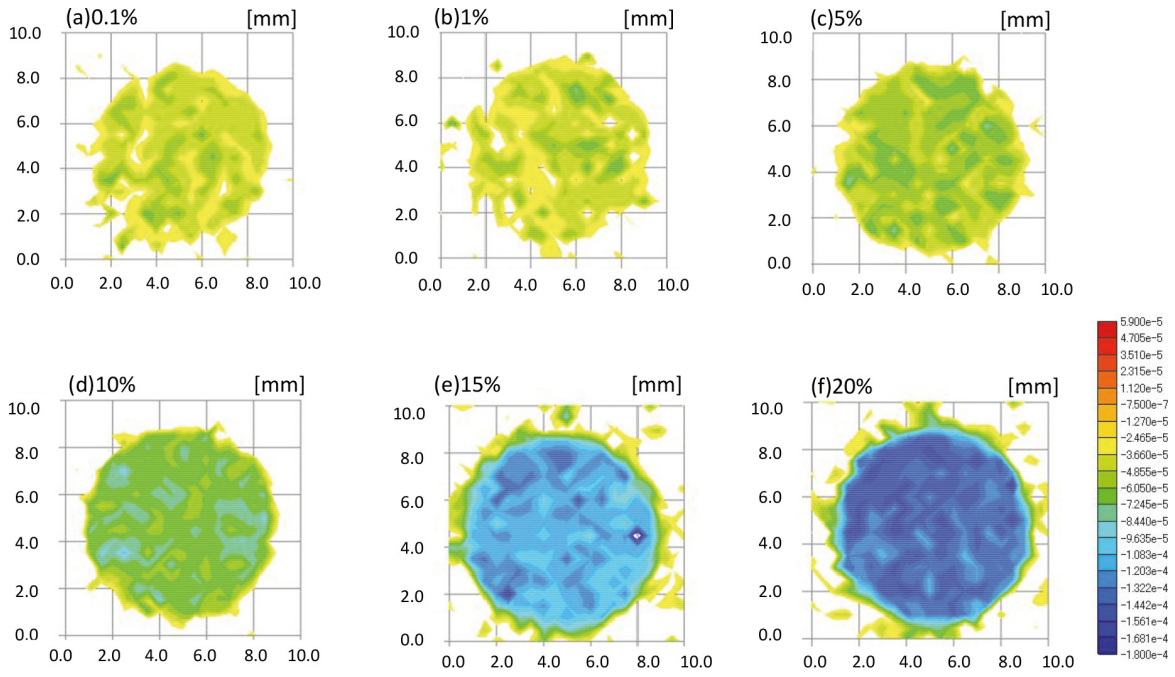

Figure 3. NIR images of tablets with different concentration of Mg-stearate developed by second derivative at 1213 nm. The numbers of (a–f) indicate the concentration of Mg-stearate.

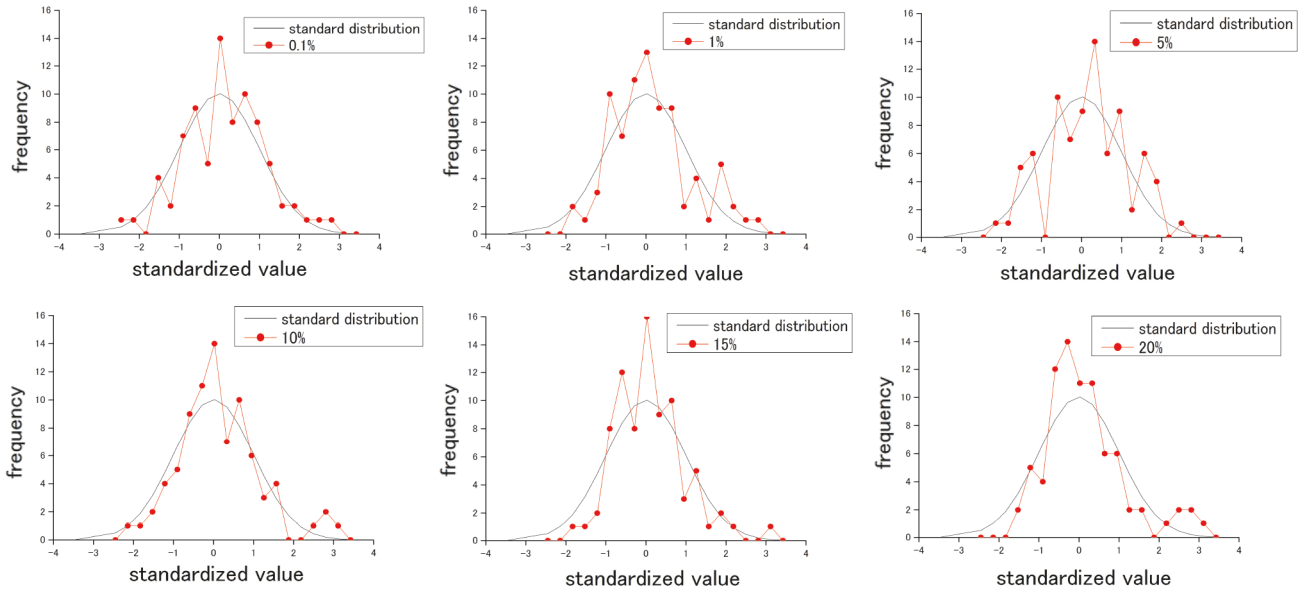

Figure 4. Frequency of standardised value obtained from second derivative spectra of sample tablets containing 0.1–20 % of Mg-stearate and standard distribution.

with the moving window method.[40] The moving window PLS method was a procedure to determine an appropriate wavelength interval selection method combined with PLS regression. The series of PLS models were built according to a window that moves over the entire spectral region, statistically determining each appropriate PLS model. Although the accuracy was slightly lower than that of previous work,[41] the result of quantitative analysis revealed that practical application of the spectral data obtained from the D-NIRs is viable.

Table 1. Summary of goodness-of-fit test for non-defective tablet containing 0.1–20 % Mg-stearate.

Concentration (%)	Replication	Statistic χ^2
0.1	1	12.09
0.1	2	19.56
0.1	3	17.13
1	1	14.31
1	2	10.87
1	3	25.47
5	1	14.61
5	2	18.13
5	3	25.17
10	1	12.86
10	2	11.75
10	3	23.8
15	1	18.28
15	2	16.79
15	3	21.86
20	1	19.71
20	2	22.92
20	3	26.35

Identification method of defective tablets

The NIR images of defective tablets developed by the second derivative method at 1213 nm are shown in Figure 5. It can be deduced that the intensity in a defective tablet is higher than that of the normal tablet. Figure 6 depicts histograms of the standard values of a defective tablet and a non-defective tablet. It was confirmed that intensity in the non-defective tablet follows the standard distribution; namely, the standardised image might be more effective to identify the defective tablet than the second derivative. Figure 7 shows standardised images of defective tablets. As expected, a part of the defect in a tablet was extracted, and the localisation of the component was more clearly identified. On the other hand, the distribution of the defective tablet was biased to the right side as compared to the normal tablet. The skewness of intensity distribution in defective and non-defective

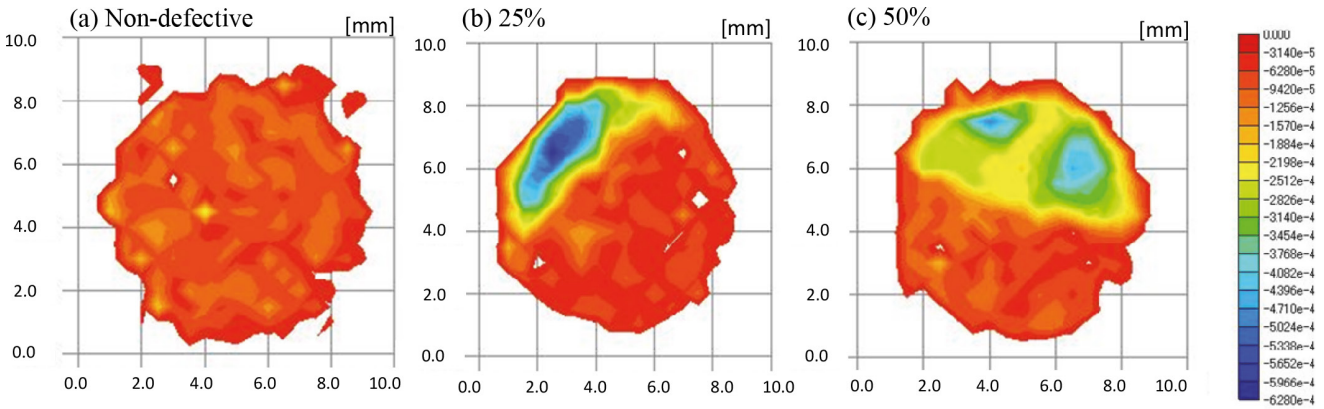

Figure 5. NIR images of (a) non-defective tablet and (b and c) defective tablets of 25 % and 50 % Mg-stearate developed by second derivative at 1213 nm. Note that the 25 % and 50 % indicate the percentage of defective area in a tablet.

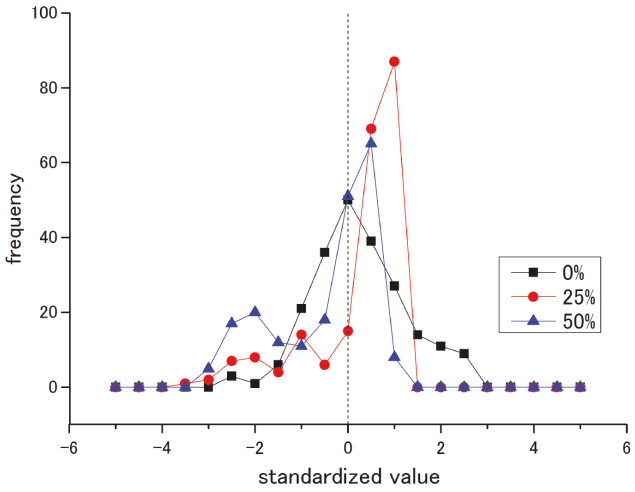

Figure 6. Frequency of standardised value obtained from second derivative at 1213 nm in a sample tablet and standard distribution. Note that the 25 % and 50 % indicate the percentage of defective area in a tablet.

tablets is depicted in Figure 8. The skewness of a normal tablet was approximately 0, and it reached approximately −2.3 in the defective tablet, which had a 12.5 % redundant concentration area. The skewness decreased gradually as the redundant concentration area increased. Therefore, if the threshold is determined, the defective tablets can be identified by the skewness of spectra. At the same time, the result suggests that the use of mean spectra can be misinterpreted, which leads to potential misidentification of defective tablets such as those prepared in this study. Moreover, the skewness with a 50 % redundant concentration area was lower than that with 25 %. Thus, the increase in the redundant portion, being more homogeneous, reduced the inhomogeneity of the tablet. As investigated by a previous study,[19] in general, kurtosis (which is the fourth-order moment about the mean) is investigated simultaneously. In the present study, the behaviour of kurtosis was similar to that of skewness

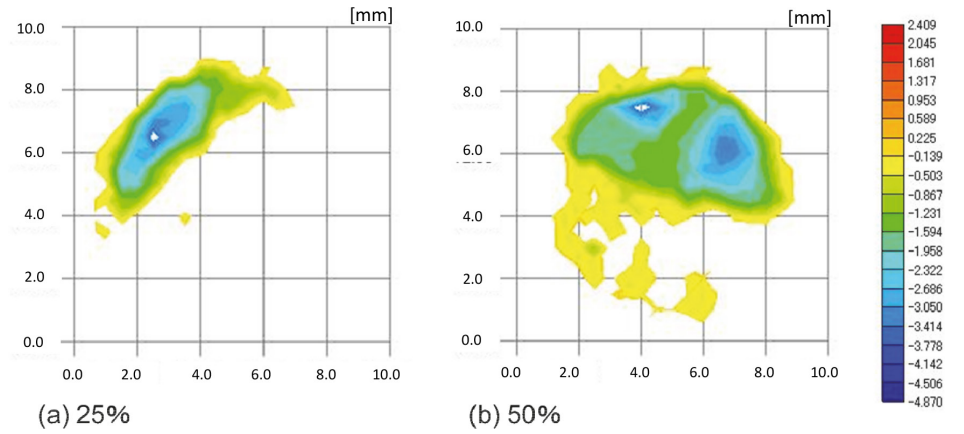

Figure 7. The standardised images of defective tablets with (a) 25 % and (b) 50 % Mg-stearate. Note that 25 % and 50 % indicate the percentage of defective area in a tablet.

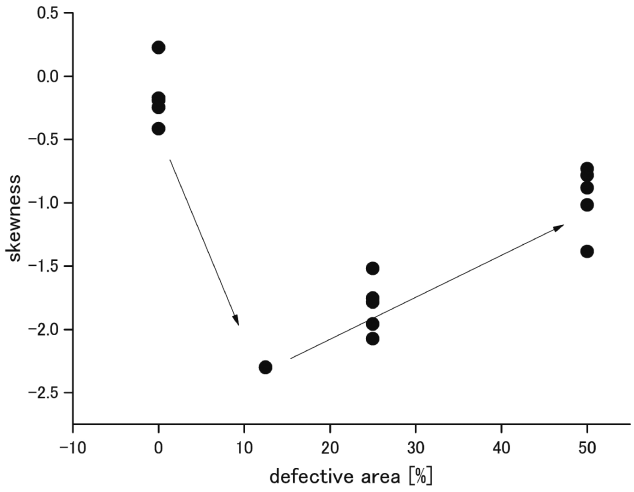

Figure 8. Change in skewness according to the increase of defective area in the tablet.

(data not shown). Because the kurtosis varies positively, in future studies, the skewness will be a more effective index as an identification method of the defective tablet.

Conclusion

This study was performed to propose a method to identify a defective tablet by NIR imaging using a newly developed imaging system, D-NIRs. Non-defective (normal) tablets with ⌀8.0 mm and 1.0 mm thickness containing 5 % ascorbic acid, 0.1–20 % Mg-stearate, 5 % talc and corn starch were prepared, and NIR spectra in the 900–1700 nm region were measured with a 1.25 nm interval and 0.5 mm spatial resolution.

The informative peak of Mg-stearate was confirmed at 1213 nm, which is due to CH stretching and NIR imaging of Mg-stearate was developed by the second derivative at 1213 nm. The distribution characteristics of an image were investigated by the goodness-of-fit test. The resulting values could not reject the null hypothesis of the test statistic with significance level $\alpha = 0.05$; thus, the distribution of non-defective tablets could be described as a normal distribution independent of the concentration. Consequently, the concentration of Mg-stearate could be predicted with $R^2 = 0.931$ and RMSE = 1.78 %. The defective tablets with localised Mg-stearate were measured, and NIR images were developed using the standardised values of second derivative spectra. The histogram of the defective tablet shifted to the right with increase in the defective area as compared to the standard distribution. The skewness of defective tablets reached −2.3, and for all defective tablets in this study, it was significantly lower than that of the normal tablet. In other words, it was shown that tablet quality can be quantified by skewness. Thus, the results obtained in this study demonstrated that the skewness of a standardised image is useful for identifying a defective tablet by NIR imaging.

References

1. K.A. Bakeev, *Process Analytical Technology*. Blackwell Publishing, Oxford, UK (2005).
2. International Conference on Harmonisation of Technical Requirements for Registration of Pharmaceuticals for Human Use, *ICH Harmonized Tripartite Guideline Pharmaceutical Development Q8 (R2)*. http://www.ich.org/fileadmin/Public_Web_Site/ICH_Products/Guidelines/Quality/Q8_R1/Step4/Q8_R2_Guideline.pdf [accessed 15 January 2015].
3. S. Laske, A. Paudel, O. Scheibelhofer, S. Sacher, T. Hoermann, J. Khinast, A. Kelly, J. Rantannen, O. Korhonen, F. Stauffer, F. De Leersnyder, T. De Beer, J. Mantanus, P.-F. Chavez, B. Thoorens, P. Ghiotti, M. Schubert, P. Tajarobi, G. Haeffler, S. Lakio, M. Fransson, A. Sparen, S. Abrahmsen-Alami, S. Folestad, A. Funke, I. Backx, B. Kavsek, F. Kjell, M. Michaelis, T. Page, J. Palmer, A. Schaepman, S. Sekulic, S. Hammond, B. Braun and B. Colegrove, "A review of PAT strategies in secondary oral dosage manufacturing of small molecules", *J. Pharm. Sci.* **106,** 667 (2017). https://doi.org/10.1016/j.xphs.2016.11.011
4. M. Fonteyne, J. Vercruysse, F. De Leersnyder, B. Van Snick, C. Vervaet, J.P. Remon and T. De Beer, "Process analytical technology for continuous manufacturing of solid-dosage forms", *Trends Anal. Chem.* **67,** 159 (2015). https://doi.org/10.1016/j.trac.2015.01.011
5. S. Šašić and Y. Ozaki, *Raman, Infrared, and Near-Infrared Chemical Imaging*. John Wiley & Sons Ltd, Hoboken, NJ (2009).
6. A.V. Ewing and S.G. Kazarian, "Recent advances in the applications of vibrational spectroscopic imaging and mapping to pharmaceutical formulations", *Spectrochim. Acta A* **197,** 10 (2018). https://doi.org/10.1016/j.saa.2017.12.055

7. R. Salzer and H.W. Siesler, *Infrared and Raman Spectroscopic Imaging*. Wiley-VCH, Weinheim, Germany (2014).

8. S. Wartewig and R.H.H. Neubert, "Pharmaceutical applications of mid-IR and Raman spectroscopy", *Adv. Drug Deliv. Rev.* **57(8),** 1144 (2005). https://doi.org/10.1016/j.addr.2005.01.022

9. M. Jamrógiewicz, "Application of the near-infrared spectroscopy in the pharmaceutical technology", *J. Pharm. Biomed. Anal.* **66,** 1 (2012). https://doi.org/10.1016/j.jpba.2012.03.009

10. E.N. Lewis, J. Schoppelrei and E. Lee, "Near-infrared chemical imaging and the PAT initiative", *Spectroscopy* **19(4),** 28 (2004).

11. J.A. Zeitler, P.F. Taday, D.A. Newnham, M. Pepper, K.C. Gordon and T. Rades, "Terahertz pulsed spectroscopy and imaging in the pharmaceutical setting—a review", *J. Pharm. Pharmacol.* **59(2),** 209 (2007). https://doi.org/10.1211/jpp.59.2.0008

12. S. Wilczyński, R. Koprowski, P. Duda, A. Banyś and B. Błońska-Fajfrowska, "Microtomographic studies of subdivision of modified-release tablets", *Int. J. Pharm.* **511(2),** 899 (2016). https://doi.org/10.1016/j.ijpharm.2016.07.069

13. M. Možina, D. Tomaževič, F. Pernuš and B. Likar, "Automated visual inspection of imprint quality of pharmaceutical tablets", *Mach. Vis. Appl.* **24(1),** 63 (2013). https://doi.org/10.1007/s00138-011-0366-4

14. G. Reich, "Near-infrared spectroscopy and imaging: basic principles and pharmaceutical applications", *Adv. Drug Deliv. Rev.* **57(8),** 1109 (2005). https://doi.org/10.1016/j.addr.2005.01.020

15. A.A. Gowen, C.P. O'Donnell, P.J. Cullen and S.E.J. Bell, "Recent applications of chemical imaging to pharmaceutical process monitoring and quality control", *Eur. J. Pharm. Biopharm.* **69(1),** 10 (2008). https://doi.org/10.1016/j.ejpb.2007.10.013

16. J. Dubois, J.C. Wolff, J.K. Warrack, J. Schoppelrei and E.N. Lewis, "NIR chemical imaging for counterfeit pharmaceutical products analysis", *Spectroscopy* **22(2),** 40 (2007).

17. M.B. Lopes and J.-C. Wolff, "Investigation into classification/sourcing of suspect counterfeit Heptodin™ tablets by near infrared chemical imaging", *Anal. Chim. Acta* **633(1),** 149 (2009). https://doi.org/10.1016/j.aca.2008.11.036

18. O.Y. Rodionova, L.P. Houmøller, A.L. Pomerantsev, P. Geladi, J. Burger, V.L. Dorofeyev and A.P. Arzamastsev, "NIR spectrometry for counterfeit drug detection a feasibility study", *Anal. Chim. Acta* **549,** 151 (2005). https://doi.org/10.1016/j.aca.2005.06.018

19. Z. Wu, O. Tao, W. Cheng, L. Yu, X. Shi and Y. Qiao, "Visualizing excipient composition and homogeneity of Compound Liquorice Tablets by near-infrared chemical imaging", *Spectrochim. Acta A* **86,** 631 (2012). https://doi.org/10.1016/j.saa.2011.10.030

20. M. Khorasani, J.M. Amigo, C.C. Sun, P. Bertelsen and J. Rantanen, "Near-infrared chemical imaging (NIR-CI) as a process monitoring solution for a production line of roll compaction and tableting", *Eur. J. Pharm. Biopharm.* **93,** 293 (2015). https://doi.org/10.1016/j.ejpb.2015.04.008

21. N. Pavurala, X. Xu and Y.S.R. Krishnaiah, "Hyperspectral imaging using near infrared spectroscopy to monitor coat thickness uniformity in the manufacture of a transdermal drug delivery system", *Int. J. Pharm.* **523(1),** 281 (2017). https://doi.org/10.1016/j.ijpharm.2017.03.022

22. P.R. Wahl, I. Pucher, O. Scheibelhofer, M. Kerschhaggl, S. Sacher and J.G. Khinast, "Continuous monitoring of API content, API distribution and crushing strength after tableting via near-infrared chemical imaging", *Int. J. Pharm.* **518(1–2),** 130 (2017). https://doi.org/10.1016/j.ijpharm.2016.12.003

23. J.M. Amigo and C. Ravn, "Direct quantification and distribution assessment of major and minor components in pharmaceutical tablets by NIR-chemical imaging", *Eur. J. Pharm. Sci.* **37(2),** 76 (2009). https://doi.org/10.1016/j.ejps.2009.01.001

24. B. Boldrini, W. Kessler, K. Rebner and R.W. Kessler, "Hyperspectral imaging: a review of best practice, performance and pitfalls for in-line and on-line applications", *J. Near Infrared Spectrosc.* **20(5),** 483 (2012). https://doi.org/10.1255/jnirs.1003

25. F.J. Bolton, A.S. Bernat, K. Bar-Am, D. Levitz and S. Jacques, "Portable, low-cost multispectral imaging system: design, development, validation, and utilization", *J. Biomed. Opt.* **23(12),** 121612 (2018). https://doi.org/10.1117/1.JBO.23.12.121612

26. M. Ishigaki, P. Puangchit, Y. Yasui, A. Ishida, H. Hayashi, Y. Nakayama, H. Taniguchi, I. Ishimaru and Y. Ozaki, "Nonstaining blood flow imaging

using optical interference due to Doppler shift and near-infrared imaging of molecular distribution in developing fish egg embryos", *Anal. Chem.* **90(8),** 5217 (2018). https://doi.org/10.1021/acs.analchem.7b05464

27. D. Ishikawa, K. Murayama, T. Genkawa, K. Awa, M. Komiyama and Y. Ozaki, "Development of compact near infrared imaging device with high-speed and portability for pharmaceutical process monitoring", *NIR news* **23(8),** 14 (2012). https://doi.org/10.1255/nirn.1340

28. K. Murayama, T. Genkawa, D. Ishikawa, M. Komiyama and Y. Ozaki, "A polychromator-type near-infrared spectrometer with a high-sensitivity and high-resolution photodiode array detector for pharmaceutical process monitoring on the millisecond time scale", *Rev. Sci. Instrum.* **84(2),** 023104 (2013). https://doi.org/10.1063/1.4790413

29. D. Ishikawa, H. Shinzawa, T. Genkawa, S.G. Kazarian and Y. Ozaki, "Recent progress of near-infrared (NIR) imaging—development of novel instruments and their applicability for practical situations", *Anal. Sci.* **30(1),** 143 (2014). https://doi.org/10.2116/analsci.30.143

30. K. Murayama, D. Ishikawa, T. Genkawa and Y. Ozaki, "An application for the quantitative analysis of pharmaceutical tablets using a rapid switching system between a near-infrared spectrometer and a portable near-infrared imaging system equipped with fiber optics", *Appl. Spectrosc.* **72(4),** 551 (2018). https://doi.org/10.1177/0003702817752697

31. K. Murayama, D. Ishikawa, T. Genkawa, H. Sugino, M. Komiyama and Y. Ozaki, "Image monitoring of pharmaceutical blending processes and the determination of an end point by using a portable near-infrared imaging device based on a polychromator-type near-infrared spectrometer with a high-speed and high-resolution photo diode array detector", *Molecules* **20(3),** 4007 (2015). https://doi.org/10.3390/molecules20034007

32. D. Ishikawa, K. Murayama, T. Genkawa, K. Awa, M. Komiyama, S. Kazarian and Y. Ozaki, "Application of a newly developed portable NIR imaging device to monitor the dissolution process of tablets", *Anal. Bioanal. Chem.* **405,** 9401 (2013). https://doi.org/10.1007/s00216-013-7355-6

33. L. de M. França, M.F. Pimentel, S. da S. Simões, S. Grangeiro, J.M. Prats-Montalbán and A. Ferrer, "NIR hyperspectral imaging to evaluate degradation in captopril commercial tablets", *Eur. J. Pharm. Biopharm.* **104,** 180 (2016). https://doi.org/10.1016/j.ejpb.2016.05.005

34. P.Y. Sacré, C. De Bleye, P.F. Chavez, L. Netchacovitch, P. Hubert and E. Ziemons, "Data processing of vibrational chemical imaging for pharmaceutical applications", *J. Pharm. Biomed. Anal.* **101,** 123 (2014). https://doi.org/10.1016/j.jpba.2014.04.012

35. J.G. Rosas, S. Armenta, J. Cruz and M. Blanco, "A new approach to determine the homogeneity in hyperspectral imaging considering the particle size", *Anal. Chim. Acta* **787,** 173 (2013). https://doi.org/10.1016/j.aca.2013.05.040

36. A. Savitzky and M.J.E. Golay, "Smoothing and differentiation of data by simplified least squares procedures", *Anal. Chem.* **36(8),** 1627 (1964). https://doi.org/10.1021/ac60214a047

37. S. Petit, A. Decarreau, F. Martin and R. Buchet, "Refined relationship between the position of the fundamental OH stretching and the first overtones for clays", *Phys. Chem. Miner.* **31(9),** 585 (2004). https://doi.org/10.1007/s00269-004-0423-x

38. H. Liu, B. Xiang and L. Qu, "Structure analysis of ascorbic acid using near-infrared spectroscopy and generalized two dimensional correlation spectroscopy", *J. Mol. Struct.* **794(1–3),** 12 (2006). https://doi.org/10.1016/j.molstruc.2006.01.028

39. J. Smetiško and S. Miljanić, "Dissolution assessment of allopurinol immediate release tablets by near infrared spectroscopy", *J. Pharm. Biomed. Anal.* **145**, 322 (2017). https://doi.org/10.1016/j.jpba.2017.06.055

40. J.-H. Jiang, R.J. Berry, H.W. Siesler and Y. Ozaki, "Wavelength interval selection in multicomponent spectral analysis by moving window partial least-squares regression with applications to mid-infrared and near-infrared spectroscopic data", *Anal. Chem.* **74(14),** 3555 (2002). https://doi.org/10.1021/ac011177u

41. H. Nakagawa, M. Kano, S. Hasebe, T. Suzuki and N. Wakiyama, "Real-time monitoring of lubrication properties of magnesium stearate using NIR spectrometer and thermal effusivity sensor", *Int. J. Pharm.* **441(1–2),** 402 (2013). https://doi.org/10.1016/j.ijpharm.2012.11.014